Evaluation of a Nisin-Eluting Nanofiber Scaffold To Treat *Staphylococcus aureus*-Induced Skin Infections in Mice

Tiaan D. J. Heunis & leon M. T. Dicks
Department of Microbiology, University of Stellenbosch, Stellenbosch, South Africa
Carine Smith
Department of Physiological Sciences, University of Stellenbosch, Stellenbosch, South Africa

ABSTRACT

Staphylococcus aureus is a virulent pathogen and a major causative agent of superficial and invasive skin and soft tissue infections (SSSTIs). Antibiotic resistance in *S. aureus*, among other bacterial pathogens, has rapidly increased, and this is placing an enormous burden on the health care sector and has serious implications for infected individuals, especially immunocompromised patients. Alternative treatments thus need to be explored to continue to successfully treat infections caused by *S. aureus*, including antibiotic-resistant strains of *S. aureus*. In this study, an antimicrobial nanofiber wound dressing was generated by electrospinning nisin (Nisaplin) into poly(ethylene oxide) and poly(d,l-lactide) (50:50) blend nanofibers. Active nisin diffused from the nanofiber wound dressings for at least 4 days *in vitro*, as shown by consecutive transfers onto plates seeded with strains of methicillin-resistant S. aureus (MRSA). The nisin-containing nanofiber wound dressings significantly reduced *S. aureus* Xen 36 bioluminescence *in vivo* and viable cell numbers in a murine excisional skin infection model. The bacterial burden of wounds treated with nisin-containing nanofiber wound dressings was 4.3×10^2 CFU/wound, whereas wounds treated with control nanofiber wound dressings had 2.2×10^7 CFU/wound on the last day of the trial (day 7). Furthermore, the wound dressings stimulated wound closure of excisional wounds, and no adverse effects were observed by histological analysis. Nisin-containing nanofiber wound dressings have the potential to treat *S. aureus* skin infections and to potentially accelerate wound healing of excisional wounds.

INTRODUCTION

Injury to skin provides a perfect site for microbial invasion, leading to minor skin infections that can easily progress into life-threatening infections. With an infection, the processes normally associated with wound healing, i.e., homeostasis, inflammation, new tissue formation, remodelling, and maturation, are hampered (1–3). Various organisms, including Gram-positive and Gram-negative bacteria, fungi, and yeasts, have been implicated in causing skin infections (4, 5). *Staphylococcus aureus* is a virulent pathogen most commonly responsible for superficial and invasive skin and soft tissue infections (SSSTIs) (6–8). Widespread use of antibiotics has led to an increase in antibiotic resistance in *S. aureus*, among others, with the emergence of health care-associated methicillin-resistant *S. aureus* (HA-MRSA) and community-acquired MRSA (CA-MRSA) (9, 10). Vancomycin-resistant strains of *S. aureus* (VRSA) and, more recently, linezolid-resistant *S. aureus* (LRSA) have also emerged (11–14). It is thus of utmost importance to evaluate alternative antimicrobial compounds and treatment strategies targeting *S. aureus*.

Lantibiotics (lanthipeptides with antimicrobial activity) are extensively posttranslationally modified bacterial antimicrobial peptides (bacteriocins) containing unusual amino acids and *meso*-lanthionine(s) and/or β-methyllanthionine(s) (15). Nisin is the best-studied lantibiotic. Posttranslational modification of the peptide results in the dehydration of serine and threonine residues of the precursor peptide to form 2,3-didehydroalanine (DHA) and (*Z*)-2,3-didehydrobutyrine (DHB), respectively. Subsequent cyclization results in the formation of one *meso*-lanthionine (Ala-S-Ala) and four β-methyllanthionines (Abu-S-Ala) in the mature peptide (16). Nisin has a dual mode of action, as it targets the pyrophosphate moiety of the cell wall precursor lipid II and, by doing so, prevents polymerization of murein subunits during cell wall biosynthesis (16, 17). Once bound to lipid II, nisin also forms pores in the cell membrane (18). Nisin is active against various Gram-positive bacteria, including MRSA, vancomycin-resistant enterococci (VRE), heterogeneous vancomycin-intermediate *S. aureus* (hVISA), *Streptococcus pneumoniae*, and *Clostridium difficile* (19–21). It has also been shown to inhibit the outgrowth of *Bacillus spp*. and *Clostridium spp*. endospores (22, 23).

Electrospinning is a versatile technique to produce fibers with minuscule diameters (in the nanometer to micrometer range) that have high oxygen permeability, variable pore sizes, and a high surface area-to-volume ratio and are morphologically similar to the extracellular matrix (24–27). Electrospun nanofibers are thus ideal as wound dressing materials. Various compounds have been electrospun into nanofibers in order to control their release (for reviews, see references 28 and 29); however, electrospinning of bacteriocins into nanofibers and the use of such electrospun nanofibers as a drug delivery system for bacteriocins in the food and medical industries have only recently been reported (30–33).

The aim of this study was to investigate the feasibility of electrospinning commercially available nisin (Nisaplin) into nanofibers consisting of a blend of poly(ethylene oxide) (PEO) and poly(d,l-lactide) (PDLLA) to generate an antimicrobial wound dressing. The release profile of nisin and the antimicrobial activity of the nisin-containing nanofiber wound dressings were evaluated *in vitro*. Furthermore, the efficacy of the nisin-containing nanofiber wound dressings to treat *S. aureus*-induced skin infections and their ability to promote wound healing were evaluated *in vivo* in an experimental murine skin infection model.

MATERIALS AND METHODS

Materials.PDLLA (75 000 to 120,000 Da) and PEO (200,000 Da) were obtained from Sigma-Aldrich (St. Louis, MO). Nisaplin was obtained from Danisco (Copenhagen, Denmark). All other reagents were of analytical grade. Protein concentrations were determined by using the microbicinchoninic acid (BCA) kit (Pierce, Rockford, IL) as recommended by the supplier, and readings were recorded at 562 nm.

Electrospinning of nanofibers.

Nisaplin was suspended in *N*,*N*-dimethylformamide (DMF) to obtain 20 mg/ml active nisin and centrifuged (8,000 × *g*, 5 min). The supernatant, containing nisin, was used as the solvent to create a 24% (wt/vol) PEO-PDLLA (50:50) solution. The solution was heated to 40°C on a hot plate and then electrospun using a gravity system as described elsewhere (31). A constant electric field of +10 kV was applied to the polymer solution, and −5 kV was applied to the collector. The collector was placed 15 cm from the polymer solution. The relative humidity was kept constant, between 50 and 54%, and the temperature was between 28 and 30°C. Nisin-containing nanofibers are referred to here as NF. Nanofibers electrospun without nisin, which served as a control, are referred to as CF.

Scanning electron microscopy of electrospun fibers.

Images of the nanofibers were recorded with a Leo 1430VP scanning electron microscope (SEM). Samples were coated with a thin layer of gold to increase conductivity. Fiber diameters were determined using the SEM Image Studio software (version 10.1), with a minimum of 100 measurements per sample from samples electrospun on three different days.

Release of nisin and *in vitro* antimicrobial activity assays.

Bioluminescent strains of *S. aureus* (Xen 29, Xen 30, Xen 31, and Xen 36; Caliper Life Sciences, Hopkinton, MA) were cultured separately in brain heart infusion (BHI) broth (Biolab Diagnostics, Midrand, South Africa) containing 200 μg/ml kanamycin to maintain the native plasmid containing the *lux* operon. Incubation was overnight at 37°C. Nisin-containing nanofibers (1 cm^2) were dissolved in DMF. The solution was then subsequently diluted in phosphate-buffered saline (PBS; pH 7.4), placed on an orbital shaker, and incubated at 37°C for 3 h. The nisin concentration was determined by using the BCA kit, as previously described. Electrospun nanofibers (1 cm^2), containing approximately 768 μg/ml nisin, were placed on the surface of seeded BHI soft agar (1%, wt/vol) plates. Into these plates was poured 20 ml BHI that was precooled before inoculation with 10^5 CFU/ml of one of the above-mentioned strains. Plates were incubated at 37°C for 24 h. Nanofibers that inhibited the growth of the *S. aureus* strains, i.e., with surrounding zones of growth inhibition, were transferred to a new plate seeded in the same way and incubated at 37°C for another 24 h. Each time, the diameter of the inhibition zone was recorded and the plates were digitally photographed. This process was repeated until no antimicrobial activity was observed.

Animals.

Approval to conduct research on animals was granted by the Ethics Committee of the University of Stellenbosch (10 NM_DIC02). Adult male BALB/c mice (weighing 20 to 30 g) were fed a standard rodent diet, housed in separate cages, and kept under controlled environmental conditions (12-h light-dark cycle; 20 to 22°C).

Skin injury and infection with *S. aureus*.

The dorsal hair of mice was removed with Veet hair remover lotion (Reckitt Benckiser, Elandsfontein, South Africa). The next day, the mice were anesthetized with 2% (vol/vol) isoflurane in O_2 (Isofor; Safe Saline Pharmaceuticals, Florida, South Africa), and full-thickness excisional wounds (5 mm in diameter) were generated on the dorsal surface of each mouse by using a sterile biopsy punch (Stellenbosch Medical Suppliers, Stellenbosch, South Africa). Mice received buprenorphine (0.03 mg/kg of body weight; Temgesic, Schering-Plough Ltd., Woodmead, South Africa) subcutaneously as an analgesic directly before injury and for the first 4 days of the experiment. *S. aureus* Xen 36 was cultured in BHI broth containing 200 μg/ml kanamycin until an optical density at 600 nm (OD_{600}) of 0.8 to 1.0 was reached. The cells were harvested by centrifugation (10,000 × *g*, 2 min) and washed once with PBS (pH 7.4). The *S. aureus* Xen 36 cells were resuspended in PBS (pH 7.4) to the same optical density and used for wound colonization. Cell counts were verified by serial dilution of the above-mentioned suspensions and plating on BHI agar plates containing 200 μg/ml kanamycin. The plates were subsequently incubated at 37°C for 24 h, after which colonies were counted. Each of the wounds was colonized with 10 μl of this 10^8-CFU/ml *S. aureus* Xen 36 suspension in PBS (pH 7.4), immediately after the punch biopsy. The cultures were placed on the wound, spread evenly using a pipette tip, and left for 10 min.

The wounds were subsequently covered with a 1-cm^2 square of parafilm, followed by a layer of gauze and Micropore surgical tape (Alpha Pharm, Stellenbosch, South Africa).

Treatment of S. *aureus* skin infections.

Treatment of the skin infections followed 1 h after wound colonization. Wounds of mice (n = 7) were covered with NF wound dressings of 1 cm^2 and were labeled as the NF group (NFG). Wounds of control mice (n = 7) were covered with CF wound dressings of the same size and were labeled the CF group (CFG). Micropore surgical tape was used to keep the nanofiber dressings in contact with the wounds. Wound dressings were changed on the second and fourth days of the 7-day trial.

Determination of bacterial bioluminescence through nanofiber wound dressings.

The signal strength of photons transmitted through the nanofiber dressings was determined prior to *in vivo* bioluminescent imaging. This was to ensure that *in vivo* bioluminescent imaging through the nanofiber dressings would be possible. Aliquots of 200 μl (10^8 CFU/ml) of *S. aureus* Xen 36 cells were placed into a microtiter plate, and the wells were covered with nanofibers, which were moistened with PBS (pH 7.4). Bioluminescent readings were recorded using the In Vivo Imaging System (IVIS 100) of Caliper Life Sciences (Hopkinton, MA). Image software (version 3.0; Caliper Life Sciences, Hopkinton, MA) was used to quantify the photons emitted from regions of interest (ROIs). The values obtained were expressed as the $\log_{10}$ of photons per second per cm^2 per steradian ($p\ s^{-1}\ cm^{-2}\ sr^{-1}$).

Monitoring the bacterial infection.

For *in vivo* bioluminescent imaging, mice were anesthetized with 2% (vol/vol) isoflurane in O_2, and bioluminescent readings were recorded, every 24 h, through the bandages for 1 min by using the IVIS 100. Nanofiber wound dressings were moistened with 50 μl PBS (pH 7.4) prior to bioluminescent imaging. Quantification of the photons emitted was achieved as described before, and the ROI area was set at 17.5 by 17.5 pixels.

Numbers of viable *S. aureus* Xen 36 cells adsorbed to the nanofiber wound dressings were determined by soaking the wound dressings in sterile saline, followed by vortexing, serial dilution, and plating on BHI plates containing 200 μg/ml kanamycin on day 2, 4, and 7. The plates were incubated at 37°C for 24 h, and the number viable cells was determined. Wounds were digitally photographed daily to investigate the influence of the wound dressings on wound closure, and images were analyzed with ImageJ software (Scion Corp., Frederick, MD). Changes in wound size were expressed as the percentage of the original wound size by using the following equation: $D_N/D_0 \times 100\%$ (D_N is the wound size on the day of measurement, and D_0 is the wound size on day zero). On day 7, the mice were euthanized with an overdose of pentabarbitone sodium (Euthapent, Kyron Laboratories Ltd., Benrose, South Africa), and wounds were excised to determine the number of viable *S. aureus* Xen 36 cells in the wounds. Excised wounds were homogenized, serially diluted in sterile saline, and plated onto BHI plates supplemented with 200 μg/ml kanamycin and incubated at 37°C for 24 h.

Effect of nanofiber wound dressings on closure of uninfected wounds.

Punch biopsies were performed on mice as previously described. None of the mice in this experiment was infected with *S. aureus*. The wounds of mice (n = 3) were covered with NF wound dressings, as described before. Wounds in control groups were either covered with CF wound dressings (n = 3) or covered only with gauze (n = 3). Micropore surgical tape was used to keep all wound dressings in

contact with the wounds. Wounds were digitally photographed daily, and wound closure was determined as described before. Wounds were excised for histological analysis on day 7 and fixed in 4% formaldehyde in 0.1 M PBS (pH 6.5). Wound tissue samples were processed by using automated procedures to impregnate and subsequently embed samples in paraffin wax; 5-μm sections were then prepared with a rotary microtome and manually stained with hematoxylin and eosin (H&E).

Statistical analysis.

Statistical analyses of the data and comparisons between groups were performed using one-way analysis of variance and/or unpaired two-tailed *t* tests. Statistica Data Analysis software (version 10; StatSoft Inc.) or GraphPad Prism software (version 5.04; GraphPad Software Inc., CA) was used. A statistically significant difference was considered when P was <0.05.

RESULTS

Electrospun nanofibers.Nanofibers electrospun from a 24% (wt/vol) solution of PEO-PDLLA (50:50) had an average diameter of 466 ± 104 nm (mean ± standard deviation), whereas nanofibers electrospun with nisin had an average diameter of 330 ± 79 nm (see Fig. S1 in the supplemental material).

In vitro activity and release profile of nisin from nanofibers.

Nisin remained active after electrospinning (Fig. 1). The highest antimicrobial activity, based on the diameters of inhibition zones, was recorded after 1 day of incubation for *S. aureus* Xen 29, MRSA Xen 30, MRSA Xen 31, and *S. aureus* Xen 36 (Fig. 1). NF wound dressings inhibited the growth of *S. aureus* Xen 29 and MRSA Xen 30 for 4 days, as observed with consecutive transfer to plates seeded with the same target organism (Fig. 1). Growth of Xen 31 was inhibited for 5 consecutive days (Fig. 1). The largest zone of growth inhibition (23 ± 1.5 mm in diameter) was recorded against *S. aureus* Xen 36 after 1 day, and growth inhibition continued for 9 consecutive days (Fig. 1). CF wound dressings did not inhibit the growth of any of the four target strains (Fig. 1). Nisin remained active in the nanofibers when stored at 4°C for 8 months. Inhibition zones of 21 ± 1.6 mm were observed after 1 day of incubation when nanofibers (which had been stored at 4°C for 8 months) were placed on plates seeded with *S. aureus* Xen 36.

Determination of bacterial bioluminescence through nanofiber wound dressings.

Bioluminescent signal slightly decreased, from 6.3 ± 0.03 to 6.2 ± 0.09 $\log_{10}$ p s^{-1} cm^{-2} sr^{-1} after transmission through moistened nanofiber wound dressings. The bioluminescent signal produced by *S. aureus* Xen 36 was thus able to transmit through PEO-PDLLA nanofiber wound dressings, which indicated that *in vivo* imaging through the nanofiber dressings was possible.

In vivo bioluminescent imaging.

NF wound dressings significantly reduced the bioluminescent signal emitted from *S. aureus* Xen 36 during 7 days of bioluminescent imaging (NFG) (Fig. 2). Mice receiving CF wound dressings (CFG), however, showed stable bioluminescence over the 7-day period. The highest bioluminescent signal recorded was on day 1 in the CFG, at 7.8 ± 0.2 $\log_{10}$ p s^{-1} cm^{-2} sr^{-1}, whereas the NFG only showed 3.9 ± 0.1 $\log_{10}$ p s^{-1} cm^{-2} sr^{-1} on day 1.

Verification of *in vivo* bioluminescent imaging by determining bacterial burdens.

The number of viable *S. aureus* cells present on NF wound dressings declined over the 7-day period. Average cell numbers per wound dressing of the NF wound dressings declined from $(2.0 \pm 1.9) \times 10^3$ on day 2 to $(1.7 \pm 4.5) \times 10^2$ and <25 CFU/wound dressing on days 4 and 7, respectively (Fig. 3A). Only 20 CFU were detected on one wound dressing (on day 7) of a mouse that was treated with NF wound dressings. Cell numbers on CF wound dressings, on the other hand, only declined from $(6.9 \pm 1.1) \times 10^7$ on day 2 to $(1.8 \pm 2.3) \times 10^6$ and $(1.2 \pm 1.5) \times 10^6$ CFU/wound dressing on days 4 and 7, respectively.

The numbers of viable *S. aureus* cells were reduced in wounds covered with NF wound dressings and were significantly lower than results in control wounds. The cell numbers of *S. aureus* Xen 36 declined to $(4.3 \pm 9.0) \times 10^2$ CFU/wound on day 7 when treated with NF wound dressings, compared to $(2.2 \pm 1.4) \times 10^7$ in wounds treated with CF wound dressings (Fig. 3B). None of the mice in the NF group had bacterial counts higher than 10^4 CFU/wound, whereas all of the mice in the CF group had cell counts higher than 10^6 CFU/wound.

Influence of nanofibers on wound healing.

No significant differences were observed in wound closure during 7 days of treatment with NF wound dressings or CF wound dressings. On average, wounds in the NF group showed an 84.0% ± 9.8% reduction in wound area on day 7, whereas wounds treated with control nanofibers showed a 79.0% ± 16.6% reduction in wound area (Fig. 4A).

A significant difference in wound area was observed in uninfected wounds covered with CF compared to wounds covered with gauze during the 7-day trial. A significant difference was, however, only observed in wound closure of mice treated with NF wound dressings compared to wounds that were covered with gauze, from day 4 until day 7 of the experiment (Fig. 4B). No difference was observed in wound closure between NF wound dressing-treated and CF wound dressing-treated wounds. Average wound sizes on day 7 ranged between 26.2% ± 3.9%, 8.7% ± 3.2%, and 9.2% ± 4.6% of the original wound area for wounds covered with gauze, CF, and NF wound dressings, respectively. Histological analysis revealed that wounds covered with gauze exhibited characteristics of reepithelialization and neovascularization in the wound bed (see Fig. S2 in the supplemental material). However, tissues surrounding the wounds showed prolonged inflammatory infiltration, with (polymorphonuclear) neutrophils still visible on day 7. Wounds treated with CF wound dressings showed signs of reepithelialization, keratinization, and wound vascularization. Some signs of neovascularization were also observed. Neutrophils were only present in one of three wounds on day 7. NF-treated wounds showed the presence of connective tissue formation, reepithelialization, keratinization, and hair follicles. None of these wounds showed any signs of neutrophil infiltration on day 7. The NF-treated group was the only group in which clear fibrotic scar formation was evident, indicating that the end stages of repair had been reached.

DISCUSSION

Skin protects the host from infection and plays a role in thermoregulation and maintenance of homeostasis; it has immunological, neurosensory, and metabolic functions. Severe skin damage exposes underlying tissue to microbial invasion (5, 34), and this delays the general wound healing process. It is thus of utmost importance to treat and/or prevent wounds from becoming infected, especially when the wounds cover a large body surface area, by using the best available treatments. In this study, a wound

dressing was generated by electrospinning nisin into PEO 50–PDLLA 50 nanofibers to generate an antimicrobial wound dressing material to target *S. aureus* skin infections.

PEO 50–PDLLA 50 nanofibers electrospun with nisin had a mean fiber diameter of 330 ± 79 nm, which corresponded well with that obtained previously (32, 35). Nanofibers electrospun without nisin had a larger diameter. Dheraprasart et al. (30), however, reported a slight increase in fiber diameter when gelatin solutions were electrospun with nisin, but the increase was not statistically significant. Various molecules and living organisms have been electrospun into a variety of natural and synthetic fibers, as well as blends thereof, including antibiotics, growth factors, antimicrobial peptides, and silver nanoparticles, as well as living bacteria (31, 36–42). Addition of molecules to a solution before electrospinning may alter the conductivity, surface tension, and possibly the viscosity of the solution and thus influence the morphology and diameter of fibers formed during electrospinning.

Antimicrobial activity was assessed on solid medium to simulate topical conditions, such as wounds. Nisin released from the PEO 50–PDLLA 50 nanofibers showed antimicrobial activity for a minimum of 4 days against *S. aureus* Xen 29 and MRSA Xen 30. The longest activity was observed against *S. aureus* Xen 36 for 9 days. An initial burst release with a sustained release of nisin was observed, which could be ideal to treat infections. Bacteria initially colonizing the wound would be killed or inhibited with the initial release of nisin, whereas the sustained release could help to prevent further infection. Similar results have been reported for bacteriocins released from nanofibers, with a high initial burst release followed by a sustained release (32). Bacteriocins released from the nanofibers inhibited the growth of a sensitive strain for up to 6 days based on antimicrobial activity on agar plates. Nisin released from electrospun gelatin nanofibers reduced *S. aureus* and *Listeria monocytogenes* numbers for over 48 h in liquid medium but was unable to reduce *Salmonella enterica* serovar Typhimurium numbers (30). Release of molecules/drugs from nanofibers, when mixed directly in the solution before electrospinning, depends on various factors, including solubility, polymer-drug interactions, and dissolution/degradation rates of the polymer/polymer blend nanofibers, as well as the experimental conditions (32, 37, 43, 44).

Survival rates of mice infected with *S. aureus* Xen 36 were 100% in both NF and CF wound dressing groups. This was ideal and offered the possibility to monitor the infection in real time as it progressed over the 7-day period with bioluminescent imaging, using the IVIS. A statistically significant reduction in bacterial bioluminescence, cell numbers on the NF wound dressings, as well as cell numbers in infected wounds were observed when treated with nisin-eluting PEO 50–PDLLA 50 nanofiber wound dressings, compared to control PEO 50–PDLLA 50 nanofiber wound dressing (CF)-treated groups. All of the mice that were treated with NF wound dressings had bacterial counts lower than 10^4 CFU/wound. Our results correlate well with previous published reports on the treatment of bacteria-infected wounds and reduction of viable cell numbers *in vivo*. Nanoemulsion compound NB-201 was shown to decrease *Pseudomonas aeruginosa* numbers in infected burn wounds from 7.9×10^7 CFU to 6.5×10^4 CFU in rats (45). Nitric oxide nanoparticles showed similar results and caused a statistically significant reduction in MRSA counts in excisional wounds (46). A proline-rich synthetic peptide, designated A3-APO, also showed potential as a treatment for burn wound infections, as it decreased the bacterial burden of wounds infected with different cell numbers of *Acinetobacter baumannii* (47). Bacterial counts of mice infected with 2×10^{11} CFU/wound were in the range of 10^7 for control animals and below 10^3 for the majority of A3-APO-treated animals (47). Further studies revealed that the peptide reduced MRSA counts in burn wounds from 10^7 to 10^4 CFU/mg of tissue and increased survival of mice infected with a cocktail of *A. baumanni*, *Klebsiella pneumoniae*, and *Proteus mirabilis* (48).

An optimal wound dressing should not just be able to treat infection but also have a beneficial effect on wound healing and speed up the process to minimize recovery time. Autografts, xenografts, and

allografts have been used in the treatment of excisional wounds. However, some problems have been identified for these treatments. These include limited availability of autografts in severely injured patients, whereas xenografts and allografts can lead to problems associated with disease transmission and immune response (49). Tissue engineering has resulted in the generation of various scaffolds to treat excisional wounds and promote wound healing. Chitosan has shown promise in the form of chitosan hydrogels and chitosan acetate bandages, as well as chitosan-(polyvinyl alcohol) nanofibers (50–52). Although the main purpose of this study was to determine if NF wound dressings could treat *S. aureus*-induced infections, the effects of the NF and CF wound dressings on wound closure were also investigated. No differences in wound closure of infected wounds treated with NF or CF wound dressings were observed. Studies have revealed that *S. aureus*-infected wounds show improved wound closure compared to uninfected or infected and treated wounds (50). However, we did not notice this effect. Even though there was no significant difference in wound closure, the wounds that were treated with NF wound dressings had a significantly lower bacterial burden than CF wound dressing-treated wounds, as previously discussed. A statistically significant difference was, however, observed for wound closure of uninfected wounds treated with NF or CF wound dressings compared to control, gauze-covered wounds. CF wound dressings, as well as NF wound dressings, showed a positive influence on wound healing, as determined by histological analysis. Hyaluronic acid nanofibers have been shown to be effective in promoting wound healing of full-thickness excisional wounds in pigs, and chitosan-poly(vinyl alcohol) nanofibers only showed a positive influence on wound healing when used in combination with R-Spondin I, a novel growth factor (52, 53). Curcumin-loaded poly(ε-caprolactone) (PCL) also showed improved wound healing from day 6 compared to plain PCL over a 10-day period in a diabetic murine model (54). Other studies have also revealed that some nanofibers do not have an added positive influence over control groups on wound closure. However, histological analysis usually reveals that the wound healing process has been stimulated more in nanofiber-treated groups (55, 56). The addition of growth factors to the nanofibers usually accelerates wound closure compared to control nanofiber-treated groups, as would be expected (52, 57).

The major factors of a nanofiber scaffold that positively influence wound healing thus seem to include the hydrophobicity/hydrophilicity ratio of the nanofiber scaffold, which will influence attachment to the wound and prevent excessive fluid buildup, and porosity, which will influence air and moisture permeability, as well as the benefit of bioactive molecules electrospun into or bound to the surface of the nanofibers (58). Our nanofiber scaffolds have good wettability and good hydrophobicity/hydrophilicity ratios; because of the blending of hydrophobic/hydrophilic polymers before electrospinning, the fibers retain the fibrous structure and their porosity upon incubation and thus have the potential as a good overall scaffold material that will positively influence wound healing (32). This was, however, a preliminary study on wound healing of uninfected wounds, and the exact influence of the nanofibers and/or nisin on wound healing warrants further investigation. It can also not be ruled out that nisin has an influence on wound healing, as cationic antimicrobial peptides play a role in the innate immune response (59). Plantaricin A, a bacteriocin produced by *Lactobacillus plantarum*, has been shown to increase cell proliferation, enhance migration, and influence the expression of transforming growth factor β1, fibroblast growth factor 7, vascular endothelial growth factor A, and interleukin-8 *in vitro* in human keratinocytes (60). Plantaricin A was shown to promote antioxidant defenses and increased the expression of *FLG*, *IVL* and *HBD-2* genes in NCTC 2544 keratinocytes (61). Decreased expression of tumor necrosis factor alpha was also observed in plantaricin A-treated cells. More recently, nisin Z was shown to have immunomodulatory activities and modulated the host immune response similarly to natural host defense peptides (62). Nisin Z mediated host protective immunity and conferred protection against Gram-positive and Gram-negative bacterial infections.

In conclusion, nisin was successfully electrospun into PEO 50–PDLLA 50 nanofibers, and released nisin was able to inhibit the growth of *S. aureus* strains over a prolonged period of time. NF wound dressings were able to significantly reduce the bacterial burden of *S. aureus*-induced skin infections in a murine model. NF and CF wound dressings were able to significantly reduce wound closure time for excisional wounds over 7 days in mice and showed no negative side effects on wound healing in a preliminary study. Nisin-containing PEO-PDLLA nanofibers can thus be suitable wound dressing materials to not only reduce the bacterial burdens of *S. aureus*-infected wounds, but also potentially decrease healing time of excisional wounds. As far as we have determined, this is the first report of an *in vivo* evaluation of an antimicrobial peptide electrospun into nanofibers to treat skin infections induced by bacteria. Future research should include the combination of growth factors, anti-inflammatory agents, and analgesics, as well as other potential antimicrobials with lantibiotics to generate an optimal wound dressing that can treat infections and reduce the time needed for wounds to heal.

FIGURES

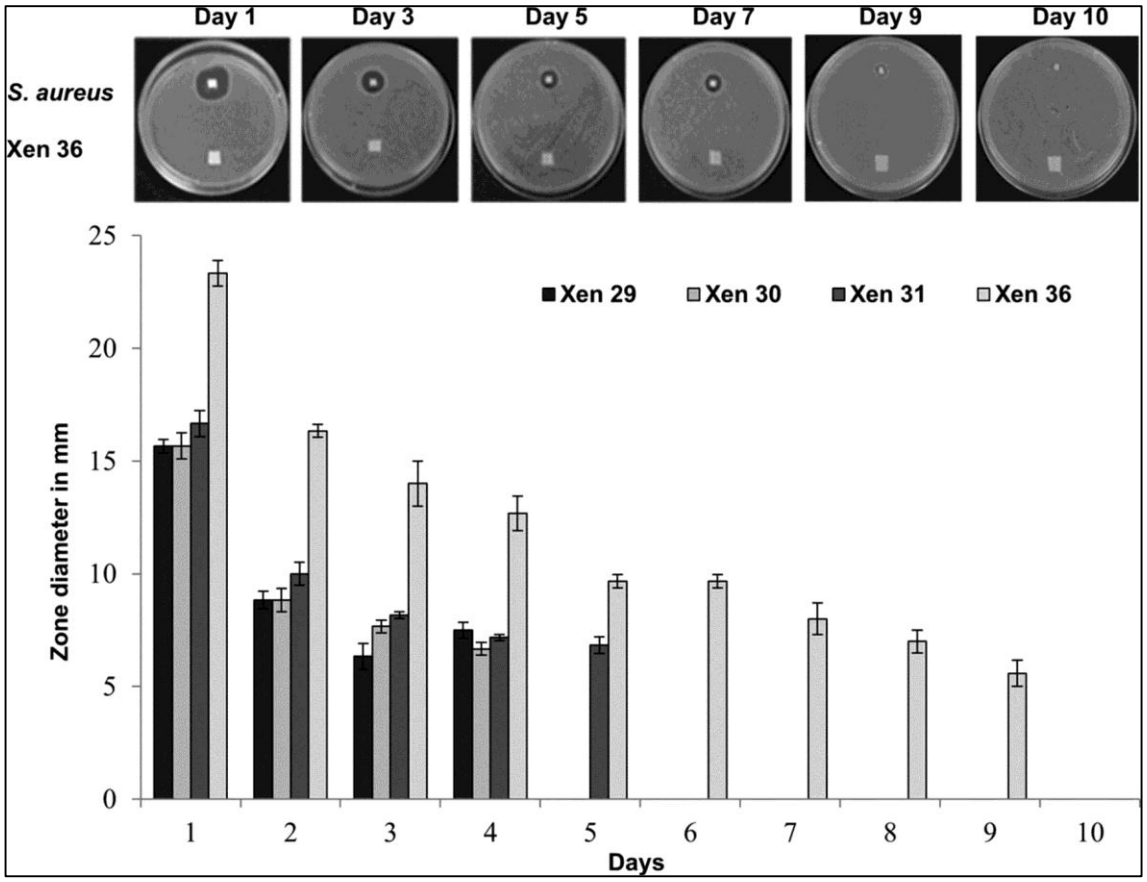

FIG 1

In vitro antimicrobial activity of nisin-eluting and control PEO 50–PDLLA 50 nanofibers against methicillin-sensitive *S. aureus* and MRSA strains. The nanofiber sample placed in the top part of the petri dish contained nisin (NF), whereas the sample placed below had no nisin (CF). The target strains of *S. aureus* were obtained from Caliper Life Sciences, Hopkinton, MA. Growth inhibition, depicted as the inhibition zone diameter, was monitored over 10 days. Error bars represent standard deviations.

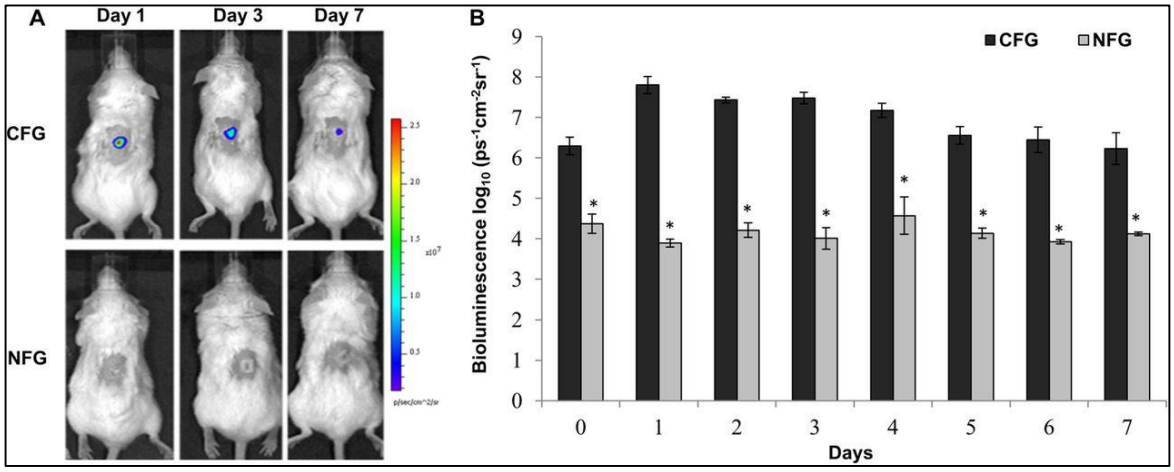

FIG 2

Efficacy of nisin-eluting PEO 50–PDLLA 50 nanofiber wound dressings to reduce *S. aureus* Xen 36 bioluminescence *in vivo* in a full-thickness excisional skin wound model in mice. Bioluminescent images (A) and bioluminescent measurements (B) of mice infected with 10 μl of 10^8 CFU/ml *S. aureus* Xen 36 and treated with nisin-containing PEO 50–PDLLA 50 nanofiber wound dressings (NFG) and control PEO 50–PDLLA 50 nanofiber wound dressings (CFG). *****, $P < 0.0001$ compared to CFG. Error bars represent standard deviations.

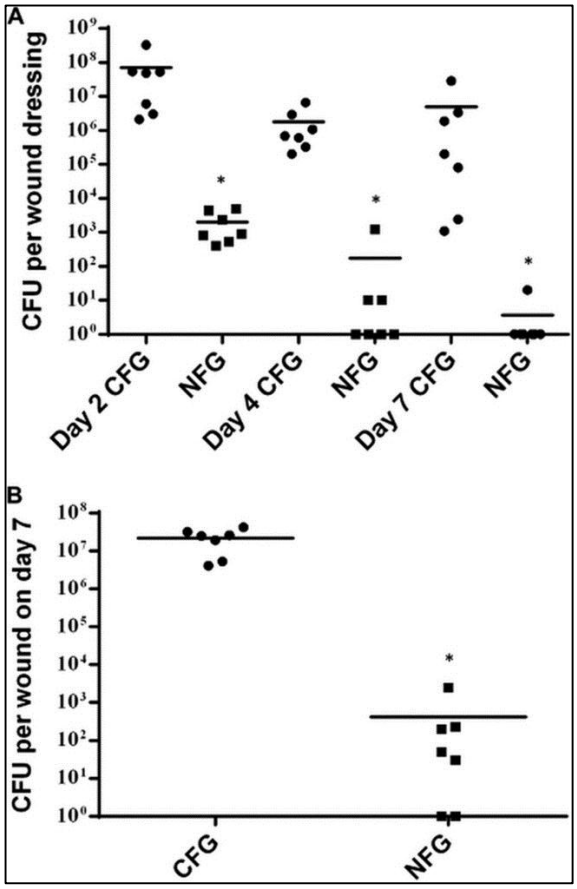

FIG 3

Efficacy of nisin-eluting PEO 50–PDLLA 50 nanofiber wound dressings in reducing bacterial (*S. aureus* Xen 36) burden in infected skin wounds as well as bacteria adsorbed to the nanofiber wound dressings. (A) CFU of *S. aureus* Xen 36 recovered from PEO 50–PDLLA 50 nanofiber wound dressings removed

from full-thickness excisional wounds on days 2, 4, and 7 of the experiment. (B) Viable *S. aureus* Xen 36 observed in excised wounds on day 7. *, $P < 0.0001$, compared to CFG on the corresponding days. Horizontal bars represent means.

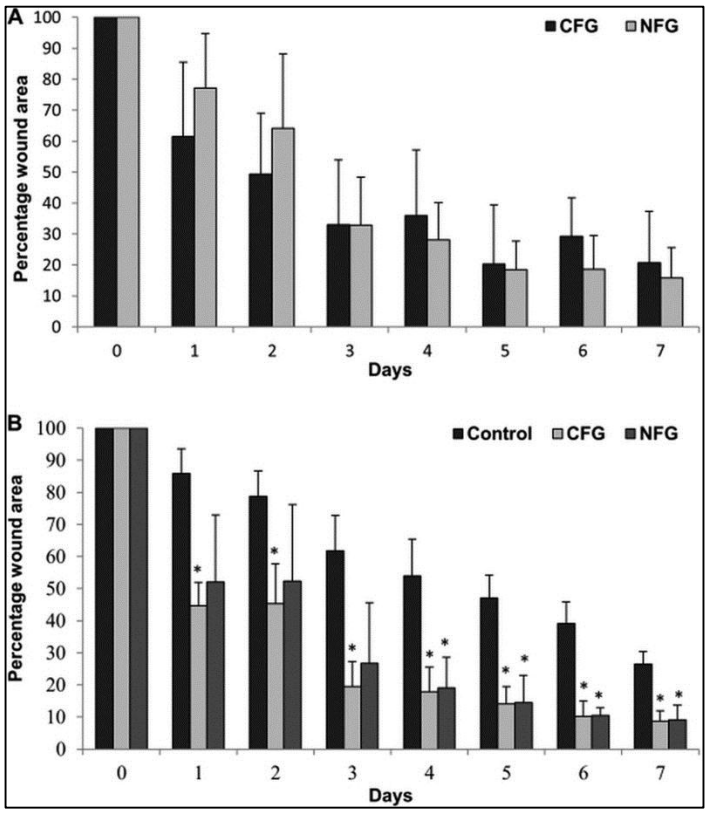

FIG 4

Influence of gauze or nisin-eluting or control PEO 50–PDLLA 50 nanofiber wound dressings on wound healing and wound closure of infected and noninfected full-thickness excisional skin wounds in mice. Full-thickness excisional wounds in mice were generated by punch biopsy and infected with 10 μl of 10^8 CFU/ml *S. aureus* Xen 36 (A) or were left uninfected (B) and subsequently covered with the different wound dressings. *, $P < 0.05$, compared to the gauze-treated group. Error bars represent standard deviations.

ACKNOWLEDGMENTS

We thank the National Research Foundation (NRF) of South Africa and Cipla Medpro Ltd. for financial support and funding of this research.

We also thank Noël Markgraaf for assistance with animals and Ashwin Isaacs for technical assistance with sample preparation and microtome sectioning.

REFERENCES

1. Guo S, DiPietro LA . *2010. Factors affecting wound healing. J. Dent. Res. 89:219–229.*
2. Gurtner GC, Werner S, Barrandon Y, Longaker MT . *2008. Wound repair and regeneration. Nature 453:314–321.*
3. Nishio N, Okawa Y, Sakurai H, Isobe K . *2008. Neutrophil depletion delays wound repair in aged mice. Age 30:11–19.*
4. Church D, Elsayed S, Reid O, Winston B, Lindsay R . *2006. Burn wound infections. Clin. Microbiol. Rev. 19:403–434.*
5. Vindenes H, Bjerknes R . *1995. Microbial colonization of large wounds. Burns 21:575–579.*
6. Baggett HC, Hennessy TW, Leman R, Hamlin C, Bruden D, Reasonover A, Martinez P, Butler JC . *2003. An outbreak of community-onset methicillin-resistant Staphylococcus aureus skin infections in southwestern Alaska. Infect. Control Hosp. Epidemiol. 24:397–402.*
7. Daum RS . *2007. Skin and soft-tissue infections caused by methicillin-resistant Staphylococcus aureus. N. Engl. J. Med. 357:380–390.*
8. Fridkin SK, Hageman JC, Morrison M, Sanza LT, Como-Sabetti K, Jernigan JA, Harriman K, Harrison LH, Lynfield R, Farley MM . *2005. Methicillin-resistant Staphylococcus aureus disease in three communities. N. Engl. J. Med. 352:1436–1444.*
9. Kim JY . *2009. Understanding the evolution of methicillin-resistant Staphylococcus aureus. Clin. Microbiol. Newsl. 31:17–23.*
10. Naimi TS, LeDell KH, Como-Sabetti K, Borchardt SM, Boxrud DJ, Etienne J, Johnson SK, Vandenesch F, Fridkin S, O'Boyle C, Danila RN, Lynfield R . *2003. Comparison of community- and health care-associated methicillin-resistant Staphylococcus aureus infection. JAMA 290:2976–2984.*
11. Chang S, Sievert DM, Hageman JC, Boulton ML, Tenover FC, Downes FP, Shah S, Rudrik JT, Pupp GR, Brown WJ, Cardo D, Fridkin SK . *2003. Infection with vancomycin-resistant Staphylococcus aureus containing the vanA resistance gene. N. Engl. J. Med. 348:1342–1347.*
12. Endimiani A, Blackford M, Dasenbrook EC, Reed MD, Bajaksouszian S, Hujer AM, Rudin SD, Hujer KM, Perreten V, Rice LB, Jacobs MR, Konstan MW, Bonomo RA . *2011. Emergence of linezolid-resistant Staphylococcus aureus after prolonged treatment of cystic fibrosis patients in Cleveland, Ohio. Antimicrob. Agents Chemother. 55:1684–1692.*
13. Tsiodras S, Gold HS, Sakoulas G, Eliopoulos GM, Wennersten C, Venkataraman L, Moellering RC, Ferraro MJ . *2001. Linezolid resistance in a clinical isolate of Staphylococcus aureus. Lancet 358:207–208.*
14. Walsh C . *1999. Deconstructing vancomycin. Science 284:442–443.*
15. Arnison PG, Bibb MJ, Bierbaum G, Bowers AA, Bugni TS, Bulaj G, Camarero JA, Campopiano DJ, Challis GL, Clardy J, Cotter PD, Craik DJ, Dawson M, Dittmann E, Donadio S, Dorrestein PC, Entian KD, Fischbach MA, Garavelli JS, Göransson U, Gruber CW, Haft DH, Hemscheidt TK, Hertweck C, Hill C, Horswill AR, Jaspars M, Kelly WL, Klinman JP, Kuipers OP, Link AJ, Liu W, Marahiel MA, Mitchell DA, Moll GN, Moore BS, Müller R, Nair SK, Nes IF, Norris E, Olivera BM, Onaka H, Patchett ML, Piel J, Reaney MJ, Rebuffat S, Ross RP, Sahl HG, Schmidt EW, Selsted ME, Severinov K, Shen B, Sivonen K, Smith L, Stein T, Süssmuth RD, Tagg JR, Tang GL, Truman AW, Vederas JC, Walsh CT, Walton JD, Wenzel SC, Willey JM, van der Donk WA . *2013. Ribosomally synthesized and post-translationally modified peptide natural products: overview and recommendations for a universal nomenclature. Nat. Prod. Rep. 30:108–160.*
16. Willey JM, van der Donk WA . *2007. Lantibiotics: peptides of diverse structure and function. Annu. Rev. Microbiol. 61:477–501.*
17. Hsu ST, Breukink E, Tischenko E, Lutters MA, de Kruijff B, Kaptein R, Bonvin AM, van Nuland NA . *2004. The nisin-lipid II complex reveals a pyrophosphate cage that provides a blueprint for novel antibiotics. Nat. Struct. Mol. Biol. 11:963–967.*

18. Brötz H, Josten M, Wiedemann I, Schneider U, Götz F, Bierbaum G, Sahl HG . *1998. Role of lipid-bound peptidoglycan precursors in the formation of pores by nisin, epidermin and other lantibiotics. Mol. Microbiol. 30:317–327.*
19. Bartoloni A, Mantella A, Goldstein BP, Dei R, Benedetti M, Sbaragli S, Paradisi F . *2004. In-vitro activity of nisin against clinical isolates of Clostridium difficile. J. Chemother. 16:119–121.*
20. Piper C, Hill C, Cotter PD, Ross RP. *2011. Bioengineering of a nisin A-producing Lactococcus lactis to create isogenic strains producing the natural variants nisin F, Q, and Z. Microb. Biotechnol. 4:375–382.*
21. Severina E, Severin A, Tomasz A . *1998. Antibacterial efficacy of nisin against multidrug-resistant Gram-positive pathogens. J. Antimicrob. Chemother. 41:341–347.*
22. Rayman MK, Aris B, Hurst A . *1981. Nisin: a possible alternative or adjunct to nitrite in the preservation of meats. Appl. Environ. Microbiol. 41:375–380.*
23. Gut IM, Blanke SR, van der Donk WA . *2011. Mechanisms of inhibition of Bacillus anthracis spore outgrowth by the lantibiotic nisin. ACS Chem. Biol. 6:744–752.*
24. Li WJ, Laurencin CT, Caterson EJ, Tuan RS, Ko FK . *2002. Electrospun nanofibrous structure: a novel scaffold for tissue engineering. J. Biomed. Mater. Res. 60:613–621.*
25. Smith LA, Ma PX . *2004. Nano-fibrous scaffolds for tissue engineering. Colloids Surf. B Biointerfaces 39:125–131.*
26. Yang F, Murugan R, Wang S, Ramakrishna S. *2005. Electrospinning of nano/micro scale poly(L-lactic acid) aligned fibers and their potential in neural tissue engineering. Biomaterials 26:2603–2610.*
27. Zhou Y, Yang D, Chen X, Xu Q, Lu F, Nie J. *2008. Electrospun water-soluble carboxyethyl chitosan/poly(vinyl alcohol) nanofibrous membrane as potential wound dressing for skin regeneration. Biomacromolecules 9:349–354.*
28. Agarwal S, Wendorff JH, Greiner A. *2008. Use of electrospinning technique for biomedical applications. Polymer 49:5603–5621.*
29. Meinel AJ, Germershaus O, Luhmann T, Merkle HP, Meinel L. *2012. Electrospun matrices for localized drug delivery: current technologies and selected biomedical applications. Eur. J. Pharm. Biopharm. 81:1–13.*
30. Dheraprasart C, Rengpipat S, Supaphol P, Tattiyakul J. *2009. Morphology, release characteristics, and antimicrobial effect of nisin-loaded electrospun gelatin fiber mat. J. Food Prot. 72:2293–2300.*
31. Heunis TDJ, Botes M, Dicks LMT. *2010. Encapsulation of Lactobacillus plantarum 423 and its bacteriocin in nanofibers. Probiotics Antimicrob. Proteins 2:46–51.*
32. Heunis T, Bshena O, Klumperman B, Dicks L. *2011. Release of bacteriocins from nanofibers prepared with combinations of poly(D,L-lactide) (PDLLA) and poly(ethylene oxide) (PEO). Int. J. Mol. Sci. 12:2158–2173.*
33. Torres NI, Sutyak Noll S, Xu S, Li J, Huang Q, Sinko PJ, Wachsman MB, Chikindas ML. *2013. Formulation and in vitro antiviral activity of the antimicrobial peptide subtilosin against herpes simplex virus type 1. Probiotics Antimicrob. Proteins 5:26–35.*
34. Altoparlak U, Erol S, Akcay MN, Celebi F, Kadanali A. *2004. The time-related changes of antimicrobial resistance patterns and predominant bacterial profiles of burn wounds and body flora of burned patients. Burns 30:660–664.*
35. Heunis TDJ. *2012. Development of an antimicrobial wound dressing by co-electrospinning bacteriocins of lactic acid bacteria into polymeric nanofibers. PhD thesis. University of Stellenbosch, Stellenbosch, South Africa.*
36. Chew SY, Wen J, Yim EKF, Leong KW. *2005. Sustained release of proteins from electrospun biodegradable fibers. Biomacromolecules 6:2017–2024.*
37. Kenawy ER, Bowlin GL, Mansfield K, Layman J, Simpson DG, Sanders EH, Wnek GE. *2002. Release of tetracycline hydrochloride from electrospun poly(ethylene-co-vinylacetate), poly(lactic acid), and a blend. J. Control. Release 81:57–64.*
38. Kim K, Luu YK, Chang C, Fang D, Hsiao BS, Chu B, Hadjiargyrou M. *2004. Incorporation and controlled release of a hydrophilic antibiotic using poly(lactide-co-glycolide)-based electrospun nanofibrous scaffolds. J. Control. Release 98:47–56.*

39. López-Rubio A, Sanchez E, Sanz Y, Lagaron JM. *2009. Encapsulation of living Bifidobacteria in ultrathin PVOH electrospun fibers. Biomacromolecules 10:2823–2829.*
40. Luu YK, Kim K, Hsiao BS, Chu B, Hadjiargyrou M. *2003. Development of a nanostructured DNA delivery scaffold via electrospinning of PLGA and PLA-PEG block copolymers. J. Control. Release 89:341–353.*
41. Maretschek S, Greiner A, Kissel T. *2008. Electrospun biodegradable nanofiber nonwovens for controlled release of proteins. J. Control. Release 127:180–187.*
42. Rujitanaroj P, Pimpha N, Supaphol P. *2008. Wound-dressing materials with antibacterial activity from electrospun gelatin fiber mats containing silver nanoparticles. Polymer 49:4723–4732.*
43. Kim TG, Lee DS, Park TG. *2007. Controlled protein release from electrospun biodegradable fiber mesh composed of poly(ε-caprolactone) and poly(ethylene oxide). Int. J. Pharm. 338:276–283.*
44. Zeng J, Xu X, Chen X, Liang Q, Bian X, Yang L, Jing X. *2003. Biodegradable electrospun fibers for drug delivery. J. Control. Release 92:227–231.*
45. Hemmila MR, Mattar A, Taddonio MA, Arbabi S, Hamouda T, Ward PA, Wang SC, Baker JR Jr. *2010. Topical nanoemulsion therapy reduces bacterial wound infection and inflammation after burn injury. Surgery 148:499–509.*
46. Martinez LR, Han G, Chacko M, Mihu MR, Jacobson M, Gialanella P, Friedman AJ, Nosanchuk JD, Friedman JM. *2009. Antimicrobial and healing efficacy of sustained release nitric oxide nanoparticles against Staphylococcus aureus skin infection. J. Investig. Dermatol. 129:2463–2469.*
47. Ostorhazi E, Rozgonyi F, Sztodola A, Harmos F, Kovalszky I, Szabo D, Knappe D, Hoffman R, Cassone M, Wade JD, Bonomo RA, Otvos L Jr. *2010. Preclinical advantages of intramuscularly administered peptide A3-APO over existing therapies in Acinetobacter baumannii wound infections. J. Antimicrob. Chemother. 65:2416–2422.*
48. Ostorhazi E, Holub MC, Rozgonyi F, Harmos F, Cassone M, Wade JD, Otvoss L Jr. *2011. Broad-spectrum antimicrobial efficacy of peptide A3-APO in mouse models of multidrug-resistant wound and lung infections cannot be explained by in vitro activity against the pathogens involved. Int. J. Antimicrob. Agents 37:480–484.*
49. Kumbar SG, Nukavarapu SP, James R, Nair LS, Laurecin CT. *2008. Electrospun poly(lactic acid-co-glycolic acid) scaffolds for skin tissue engineering. Biomaterials 29:1400–1407.*
50. Burkatovskaya M, Castano AP, Demidov-Rice TN, Tegos GP, Hamblin MR. *2008. Effect of chitosan acetate bandage on wound healing in infected and noninfected wounds in mice. Wound Repair Regen. 16:425–431.*
51. Kiyozumi T, Kanatani Y, Ishihara M, Saitoh D, Shimizu J, Yura H, Suzuki S, Okada Y, Kikuchi M. *2007. The effect of chitosan hydrogel containing DMEM/F12 medium on full-thickness skin defects after deep dermal burn. Burns 33:642–648.*
52. Sundaramurthi D, Vasanthan KS, Kuppan P, Krishnan UM, Sethuraman S. *2012. Electrospun nanostructured chitosan-poly(vinyl alcohol) scaffolds: a biomimetic extracellular matrix as dermal substitute. Biomed. Mater. 7:1–12.*
53. Uppal R, Ramaswamy GN, Arnold C, Goodband R, Wang Y. *2011. Hyaluronic acid nanofiber wound dressing-production, characterization, and in vivo behaviour. J. Biomed. Mater. Res. B Appl. Biomater. 97B:20–29.*
54. Merrell JG, McLaughlin SW, Tie L, Laurecin CT, Chen AF, Nair LS. *2009. Curcumin-loaded poly(ε-caprolactone) nanofibres: diabetic wound dressing with antioxidant and anti-inflammatory properties. Clin. Exp. Pharmacol. Physiol. 36:1149–1156.*
55. Liu X, Lin T, Fang J, Yao G, Zhao H, Dodson M, Wang X. *2010. In vivo wound healing and antibacterial performances of electrospun nanofibre membranes. J. Biomed. Mater. Res. A 94A:499–508.*
56. Rho KS, Jeong L, Lee G, Seo BM, Park YJ, Hong SD, Roh S, Cho JJ, Park WH, Min BM. *2006. Electrospinning of collagen nanofibers: effects on the behaviour of normal human keratinocytes and early-stage wound healing. Biomaterials 27:1452–1461.*
57. Choi JS, Leong KW, Yoo HS. *2008. In vivo wound healing of diabetic ulcers using electrospun nanofibers immobilized with human epidermal growth factor (EGF). Biomaterials 29:587–596.*

58. Liu X, Lin T, Gao Y, Xu Z, Huang C, Yao G, Jiang L, Tang Y, Wang X. *2012. Antimicrobial electrospun nanofibers of cellulose acetate and polyester urethane composite for wound dressing. J. Biomed. Mater. Res. B Appl. Biomater. 100B:1556–1565.*
59. Barak O, Treat JR, James WD. *2005. Antimicrobial peptides: effectors of innate immunity in the skin. Adv. Dermatol. 21:357–374.*
60. Pinto D, Marzani B, Minervini F, Calasso M, Giuliani G, Gobbetti M, De Angelis M. *2011. Plantaricin A synthesized by Lactobacillus plantarum induces in vitro proliferation and migration of human keratinocytes and increases the expression of TGF-β1, FGF7, VEGF-A and IL-8 genes. Peptides 32:1815–1824.*
61. Marzani B, Pinto D, Minervini F, Calasso M, Di Cagno R, Giuliani G, Gobbetti M, De Angelis M. *2012. The antimicrobial peptide pheromone plantaricin A increases antioxidant defenses of human keratinocytes and modulates the expression of filaggrin, β-defensin 2 and tumor necrosis factor-α genes. Exp. Dermatol. 21:665–671.*
62. Kindrachuk J, Jenssen H, Elliott M, Nijnik A, Magrangeas-Janot L, Pasupuleti M, Thorson L, Ma S, Easton DM, Bains M, Finlay B, Breukink EJ, Sahl HG, Hancock REW. *2013. Manipulation of innate immunity by a bacterial secreted peptide: lantibiotic nisin Z is selectively immunomodulatory. Innate Immun. 19:315–327.*

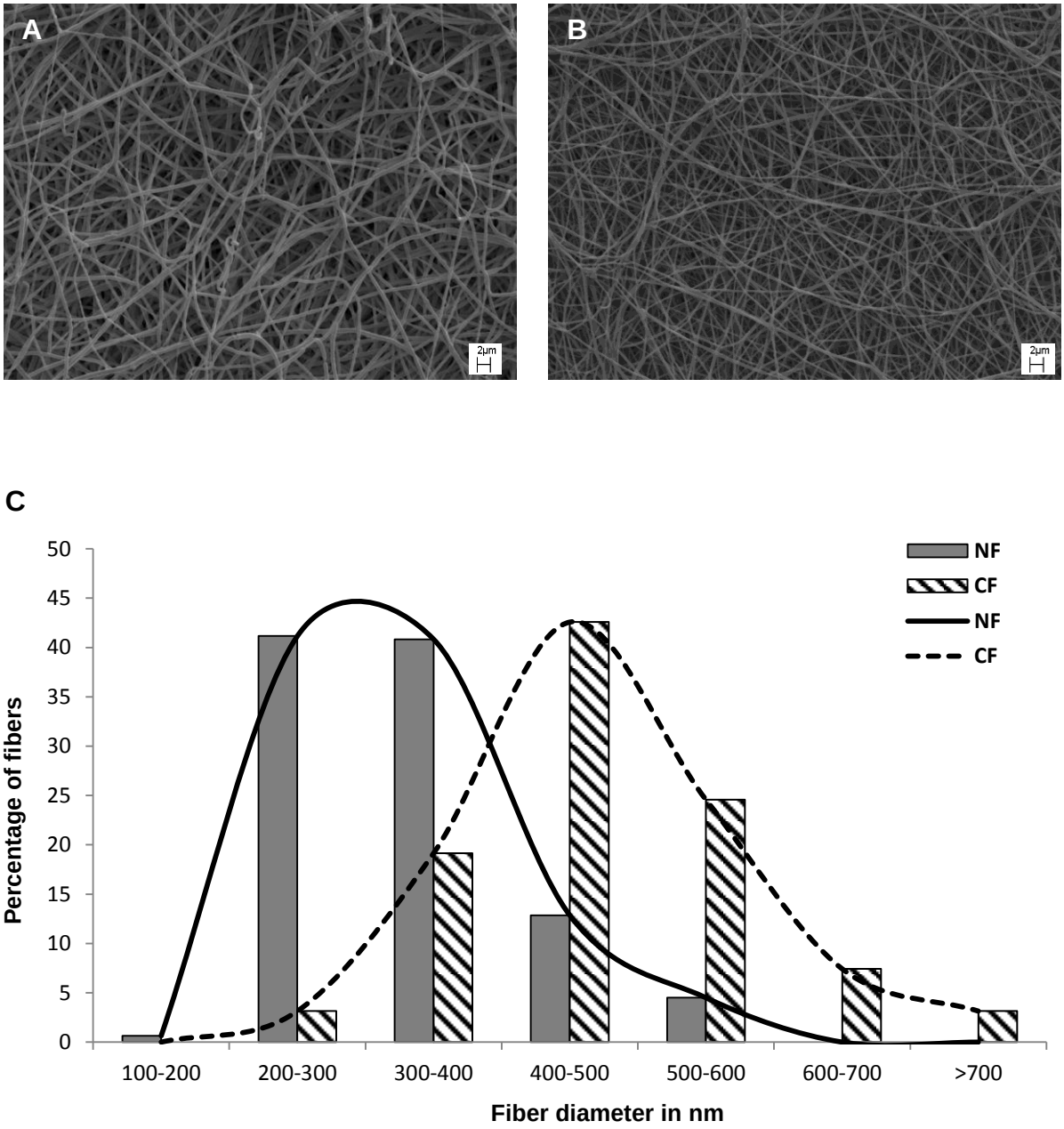

FIG S1 Scanning electron microscopy (SEM) images of nanofibers and nanofiber diameters. SEM images of PEO 50:PDLLA 50 nanofibers electrospun (A) without nisin and (B) electrospun with nisin. Distribution of nanofiber diameters in samples electrospun without nisin (CF) and with nisin (NF) are shown in (C).

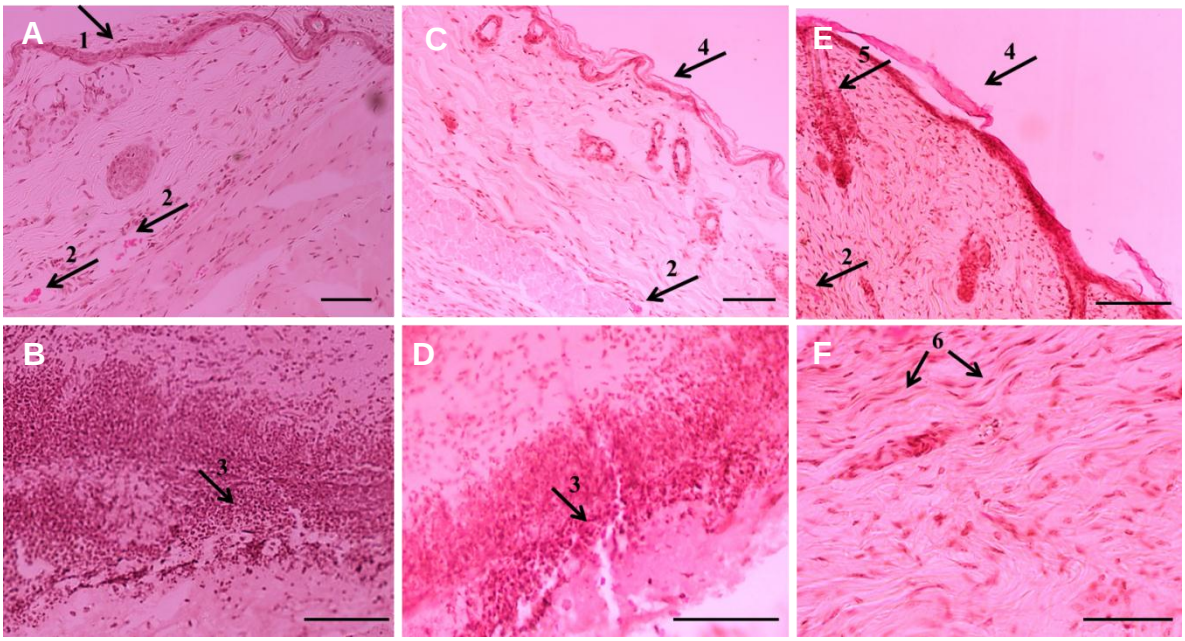

FIG S2 Histological analysis of non-infected full-thickness excisional wounds in mice covered with gauze, nisin-eluting- and control-PEO 50:PDLLA 50 nanofiber wound dressings to investigate wound healing. Skin sections (stained with H&E) of excisional wounds covered with gauze (A: wound bed and B: tissue adjacent to wound bed), control PEO 50:PDLLA 50 nanofibers (C: wound bed and D: tissue adjacent to wound bed) and nisin-containing nanofibers (E and F, both of wound bed) on day 7. 1: re-epithelialization, 2: neovascularization, 3: neutrophils, 4: keratinization, 5: hair follicle and 6: fibrosis (fibrotic scar formation). Scale bar = 20 µm.